*J. Fluid Mech.* (1996), *vol.* 319, *pp.* 305–322



# Coupled Batchelor flows in a confined cavity

By M. VYNNYCKY AND K. KANEV†

Tohoku National Industrial Research Institute, 4-2-1 Nigatake, Miyagino-Ku, Sendai, 983 Japan

(Received 30 October 1995 and in revised form 27 February 1996)

Steady, inviscid, incompressible two-dimensional flow in a quarter-circular cavity containing two vortex patches is investigated. A two-parameter family of solutions, characterized by any two out of the positions of the separation and reattachment points of the main eddy, the tangential velocity at separation and the ratio of the core vorticities, is identified and computed numerically. It is found that solutions can only be obtained for a rather narrow band of combinations of these parameters; the reasons for this constraint are discussed. Finally, we consider whether any of the coupled Batchelor flow solutions actually does represent the limit of high Reynolds number flow by comparing the inviscid results with those of earlier Navier–Stokes computations (Vynnycky & Kimura 1994). Agreement for the position of the dividing streamline and the location of the centre of the main core proves to be very encouraging, and suggestions are made as to the possible future development of such a two-eddy model.

## 1. Introduction

Inviscid flows which have uniform vorticity and are bounded by vortex sheets have received attention because they may plausibly explain the structure of viscous flow in the idealized limit of infinite Reynolds number ($Re$). Since this proposal was first made (Batchelor 1956*a*, *b*), much effort has been expended in obtaining a mathematically complete picture of high Reynolds number flow past a bluff body. In the situation where the bluff body is a circular cylinder, the wake behind the cylinder is now believed to consist of two symmetric counter-rotating eddies of constant vorticity of height and length $O(Re^{1/2})$, each separated from the irrotational mainstream flow by vortex sheets (for example, Smith 1985; Fornberg 1985). The inviscid computational aspects of this problem, namely finding the *a priori* unknown position of the vortex sheet, have been considered by Sadovskii (1971), Pierrehumbert (1980), Smith (1986) and Moore, Saffman & Tanveer (1988). Other exterior inviscid flow problems of a similar nature have also received attention, principally rotational corner flow (Chernyshenko 1984; Moore *et al.* 1988), flow past a wedge (Saffman & Tanveer 1984) and Batchelor flows in channels (Chernyshenko 1993; Turfus 1993; Giannakidis 1993). In each case, solution curves are characterized by the value of the constant core vorticity, although the boundary-layer computations which seem likely to be able to determine which value viscous theory will select have yet to be carried out.

For interior flows, on the other hand, there have been some successes in unifying quantitatively the results of high Reynolds number computations with those of the inviscid and boundary-layer theories arising from asymptotic analysis for $Re \gg 1$. In these cases, with the inviscid constant-vorticity region coincident with the enclosing

† Present address: Visual Science Laboratory, Inc., Awajicho MH bldg. 2-21 Kanda Awajicho, Chiyoda-Ku, Tokyo, 101 Japan

boundary, the measure of agreement between the two approaches is the numerical value of the core vorticity. In particular, the linearized analysis of Lyne (1970) for driven flow in a semi-circle produces good agreement with the numerical results of Kuwahara & Imai (1969), whilst the computations of Haddon & Riley (1985) for flow in a family of ellipses with varying eccentricities appear to agree, after extrapolation, with the boundary-layer methods of Riley (1981) and Vynnycky (1994).

However, interior flows containing a separated boundary layer, like the classical driven cavity problem wherein flow in a square box is driven by the uniform motion of one of its sides, have proved to be analytically intractable. Since it was first formulated (Burggraf 1966), the driven cavity has often been used a model problem for testing the effectiveness of Navier–Stokes solvers at high Reynolds number (for example, Schreiber & Keller 1983; Vanka 1986; Bruneau & Jouron 1990); it is now well-known, for instance, that flow separation occurs within the cavity, so that in addition to the main eddy, recirculating eddies develop in three corners of the box when $Re \sim O(10^4)$. The treatment of the inviscid aspects of a situation of this type, with analogy to exterior flows, thus forms the purpose of this paper. For example, were one to attempt to construct a model based on coupled Batchelor flows, one would naturally be led, based on the high Reynolds number computations just mentioned, to include three free boundaries. Rather than attempt the classical driven-cavity problem for the purposes of considering the issue of internally confined coupled Batchelor flows, we opt instead for a scenario containing just one such free boundary. Recently, Vynnycky & Kimura (1994) have considered high Reynolds number flow in a quarter-circle, driven by a constant shear at one of its flat boundaries, the other being subject to no shear; flow separation occurs at the curved no-slip boundary, resulting in a more vigorous flow on one side of the dividing streamline, with a counter-rotating eddy on the other. The boundary conditions in their problem ensure that there is only one such dividing streamline. For the inviscid flow considered in this paper, the full boundary conditions used in that paper are unimportant, except in so far as there is no normal flow out of the quarter-circle and the imposed boundary conditions for shear stress and tangential velocity are consistent with the establishment of two recirculating flows. The earlier paper considers both clockwise and anticlockwise flow, although in the latter case, the streamfunction contours indicate that the position of the dividing streamline is affected at reattachment by the viscous shear layer at the horizontal layer. Consequently, as we are seeking an inviscid model, we deal with their clockwise flow case.

In § 2, we formulate an inviscid two-eddy problem and identify the features of the Batchelor flows we might expect. In particular, there are found to be two degrees of freedom, corresponding to any two of: the separation and reattachment points of the main eddy; the ratio of the core vorticities; and the slip velocity at separation and reattachment of the main eddy. In § 3, the solution method, adapted from one of two used by Moore *et al.* (1988) and involving the iterative solution of two coupled Fredholm equations, is explained. In § 4, we present the main body of the results, while in § 5, we compare them quantitatively, where possible, with those of Vynnycky & Kimura (1994), whose computations we re-do using a finer, uniform mesh. Our findings are assessed in § 6, in particular as regards whether the two-eddy model does actually represent the high-$Re$ limit, and future extensions are proposed.

## 2. Formulation

In the region $x > 0, y > 0, x^2 + y^2 < 1$ (see figure 1), we assume there to be two Batchelor flows, given by streamfunctions $\psi_\pm$ and constant vorticities $\omega_\pm$, below and

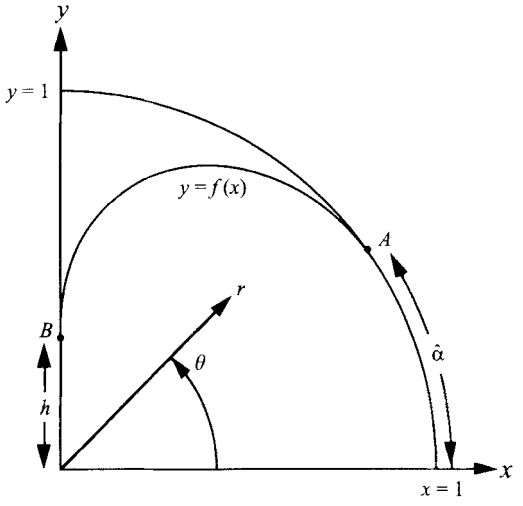


FIGURE 1. Sketch of the geometry for coupled Batchelor flows.

above, respectively, the curve $y = f(x)$. Flow separation is assumed to occur at $A$ $(\cos\hat{\alpha}, \sin\hat{\alpha})$ on $x^2 + y^2 = 1$, with reattachment at $B$ $(0, h)$, where $h = f(0)$. The governing equations for $\psi_\pm$ are then

$$\nabla^2\psi_\pm = -\omega_\pm, \tag{2.1a,b}$$

subject to

$$\psi_+ = 0 \quad \text{on} \quad \begin{cases} y = 0, \quad 0 \leqslant x \leqslant 1, \\ x = 0, \quad 0 \leqslant y \leqslant h, \\ y = f(x), \quad 0 \leqslant x \leqslant \cos\hat{\alpha}, \\ x^2 + y^2 = 1, \quad \cos\hat{\alpha} \leqslant x \leqslant 1. \end{cases} \tag{2.2a}$$

and

$$\psi_- = 0 \quad \text{on} \quad \begin{cases} x = 0, \quad h \leqslant y \leqslant 1, \\ y = f(x), \quad 0 \leqslant x \leqslant \cos\hat{\alpha}, \\ x^2 + y^2 = 1, \quad 0 \leqslant x \leqslant \cos\hat{\alpha}. \end{cases} \tag{2.2b}$$

For the configuration to be steady, the pressure $p$ must be continuous across $y = f(x)$. By Bernoulli's theorem,

$$p_\pm + \tfrac{1}{2}(\nabla\psi_\pm)^2 = C_\pm \quad \text{on} \quad y = f(x)_\pm, \tag{2.3a,b}$$

so that continuity of pressure requires

$$(\nabla\psi_+)^2 - (\nabla\psi_-)^2 = q^2, \tag{2.4}$$

where

$$q^2 = 2(C_+ - C_-) \tag{2.5}$$

and $C_\pm$ are the Bernoulli constants.

The substitutions $\psi_\pm = \omega_\pm\tilde{\psi}_\pm$ then give

$$\nabla^2\tilde{\psi}_\pm = -1, \tag{2.6a,b}$$

with $\tilde{\psi}_\pm$ satisfying (2.2*a*,*b*) respectively, and with (2.4) now

$$(\nabla\tilde{\psi}_+)^2 - \Omega^2(\nabla\tilde{\psi}_-)^2 = Q^2, \tag{2.7}$$

where

$$\Omega = \frac{\omega_-}{\omega_+}, \quad Q = \frac{q}{\omega_+}. \tag{2.8a,b}$$

Note here that it is advisable to define $\Omega$ as $\omega_-/\omega_+$, rather than $\omega_+/\omega_-$, since this permits us to deal with the hypothetical case $\omega_- = 0$, corresponding to stagnant flow in the upper region; on the other hand, since the mechanism for flow is assumed to exist at $y = 0$, we do not need to consider the eventuality $\omega_+ = 0$.

Writing

$$Q_\pm = \frac{\partial \tilde{\psi}_\pm}{\partial n},$$

then, if $Q \neq 0$, $Q_\pm$ cannot both vanish at $A$ and at $B$ and the only possibility is that $Q_+ = Q$, $Q_- = 0$, corresponding to tangential separation and reattachment. Furthermore, if $Q = 0$, an evident solution in series form is for the case $h = 0, \Omega = \pm 1$, given by

$$\tilde{\psi}_+ = \left(\frac{2\hat{\alpha}}{\pi}\right)^2 \sum_{n=1}^{\infty} \frac{(r^{\pi(2n-1)/\hat{\alpha}} - r^2)\sin(2n-1)\pi\theta/\hat{\alpha}}{(2n-1)\left((2\hat{\alpha}/\pi)^2 - (2n-1)^2\right)}, \tag{2.9a}$$

$$\tilde{\psi}_- = \left(1 - \frac{2\hat{\alpha}}{\pi}\right)^2 \sum_{n=1}^{\infty} \frac{(r^{[\pi/(\pi/2-\hat{\alpha})](2n-1)} - r^2)\sin(2n-1)[\pi(\theta-\hat{\alpha})]/(\frac{1}{2}\pi - \hat{\alpha})}{(2n-1)\left((1-2\hat{\alpha}/\pi)^2 - (2n-1)^2\right)}, \tag{2.9b}$$

with $\hat{\alpha} = \frac{1}{4}\pi$, so that $f(x) = x$, and the separation angle is $\frac{1}{2}\pi$. Using (2.9a,b), it is clear that if $Q = 0$, the separation angle must necessarily be $\frac{1}{2}\pi$; otherwise, if we suppose it to be $\beta$ (say) where, without loss of generality, $0 < \beta < \frac{1}{2}\pi$, then in terms of local polar coordinates $(r^*, \theta^*)$ taken about the separation point, we would have

$$\tilde{\psi}_+ \sim r^{*2} \sin\frac{\pi\theta^*}{\beta}, \quad \tilde{\psi}_- \sim r^{*\pi/(\pi-\beta)} \sin\frac{\pi(\theta^* - \beta)}{\pi - \beta},$$

so that in evaluating $(Q_\pm)_{\theta^*=\beta}$ for $r^* \ll 1$,

$$Q_+ \sim r^*, \quad Q_- \sim r^{*\beta/(\pi-\beta)}$$

so that locally $Q_+^2 \neq \Omega^2 Q_-^2$. Further if $Q = 0$, then $\Omega^2 = 1$ by a similar reasoning.

Whilst we are unable to provide a rigorous uniqueness theorem for the solution of the above equations when $Q \neq 0$, counting arguments for the discretized equations along the lines of Moore *et al.* (1988) indicates that if $\hat{\alpha}$ and $h$ are given, then $Q, \Omega$ and $f(x)$ can be determined. If we describe $f(x)$ by the coordinates $(x_m, y_m)$, where $m = 0, 1, .., N$, then since the separation and reattachment points are known, the unknowns are $y_1, y_2, .. y_{N-1}, Q$ and $\Omega$, a total of $N + 1$. Now, the boundary-value problems for the streamfunctions $\tilde{\psi}_\pm$ determine uniquely the velocities $Q_\pm$ at $(x_m, y_m)$, so that applying (2.7) at $(x_m, y_m)$ $(m = 0, 1, .., N)$ gives $N + 1$ equations

$$R_m \equiv Q_+^2(m) - \Omega^2 Q_-^2(m) - Q^2 = 0 \quad (m = 0, 1, .., N), \tag{2.10}$$

where

$$Q_\pm(m) = Q_\pm(x_m, y_m) \quad (m = 0, 1, .., N).$$

Note that once a solution has been found, then changing the sign of $Q$, $\Omega$ or both also produces a solution.

To consider flow near separation or reattachment, we introduce local coordinates $(s, n)$ along and perpendicular to the boundary of the quarter-circle, and consider

without loss of generality the separation point $A$. The equation for $\tilde{\psi}_-$ is then approximately

$$\frac{\partial^2 \tilde{\psi}_-}{\partial n^2} = -1, \tag{2.11}$$

whence the particular integral $\tilde{\psi}_-^{(p)}$ is approximately

$$\tilde{\psi}_-^{(p)} = -\tfrac{1}{2}(n - n_A)^2 + \tfrac{1}{2}(n - n_A)g(s - s_A), \tag{2.12}$$

where

$$n - n_A = g(s - s_A)$$

is the equation for $y = f(x)$ in the vicinity of the separation point and $g(0), g'(0)$ both vanish. Thus, as $s \to s_A$,

$$Q_- = \frac{\partial \tilde{\psi}_-^{(p)}}{\partial n} \sim o(s - s_A)^2,$$

so that

$$Q_+ = Q + o(s - s_A)^2. \tag{2.13}$$

Next, although the flow in the lower region is rotational, $\tilde{\psi}_+$ will be dominated near the separation point by an irrotational term of the form $Qn$, in which case the analysis of Smith (1982) leading to the results of Kirchhoff's free-streamline theory holds, so that

$$g(s - s_A) = a_A(s - s_A)^{3/2} + \ldots, \tag{2.14}$$

where $a_A$ is the cusp constant. This provides the necessary details near the separation point for parameterizing the solution curve in § 3.

## 3. Solution

We rearrange the foregoing into a form amenable to numerical solution; the method is based on one used by Moore *et al.* (1988), although with enough differences to warrant a detailed account. Introducing plane polar $(r, \theta)$ coordinates, related to Cartesian coordinates as usual by

$$x = r\cos\theta, \quad y = r\sin\theta,$$

and writing

$$\hat{\psi}_\pm = \tilde{\psi}_\pm - \psi_c, \tag{3.1a,b}$$

the equation

$$\begin{aligned}\psi_c(r,\theta) = (1/\pi)\Bigg(&-r^2\log r\sin 2\theta - \frac{1}{4}r^2(4\theta\cos 2\theta + \pi - \pi\cos 2\theta)\\ &+\frac{1}{8}(r^2 - 1/r^2)\sin 2\theta\log\left[(1+r^4)^2 - 4r^4\cos^2 2\theta\right]\\ &-\frac{1}{4}\left(r^2 + \frac{1}{r^2}\right)\cos 2\theta\tan^{-1}\left[\frac{r^4\sin 4\theta}{1 - r^4\cos 4\theta}\right] + \frac{1}{2}\tan^{-1}\left[\frac{2r^2\sin 2\theta}{1 - r^4}\right]\Bigg)\end{aligned} \tag{3.2}$$

can be derived as the solution to (2.6), subject to homogeneous boundary conditions on the boundary of the quarter-circle. Equation (2.6*a*,*b*) gives

$$\nabla^2\hat{\psi}_\pm = 0, \tag{3.3a,b}$$

with boundary conditions for $\hat{\psi}_+$,

$$\hat{\psi}_+ = \begin{cases} 0 & \text{on } \theta = 0,\ 0 \leqslant r \leqslant 1;\ \theta = \frac{1}{2}\pi,\ 0 \leqslant r \leqslant h;\ r = 1,\ 0 \leqslant \theta \leqslant \hat{\alpha}; \\ -\psi_c & \text{on } r = f(\theta), \end{cases} \tag{3.4a}$$

and for $\hat{\psi}_-$,

$$\hat{\psi}_- = \begin{cases} 0 & \text{on } \theta = \frac{1}{2}\pi,\ h \leqslant r \leqslant 1;\ r = 1,\ \hat{\alpha} \leqslant \theta \leqslant \frac{1}{2}\pi; \\ -\psi_c & \text{on } r = f(\theta). \end{cases} \tag{3.4b}$$

Denoting by $Q_c$ the tangential velocity due to $\psi_c$, and by $\tilde{Q}_\pm$ that due to $\tilde{\psi}_\pm$, at the dividing interface, (2.7) is now

$$\left(\tilde{Q}_+ + Q_c\right)^2 - \Omega^2 \left(\tilde{Q}_- + Q_c\right)^2 = Q^2. \tag{3.5}$$

Defining the complex variables $z$ and $Z$ by $z = x + \mathrm{i}y$ and $Z = X + \mathrm{i}Y$ respectively, consider the conformal map

$$z \longmapsto Z = \frac{(z^2+1)^2 + \tilde{\gamma}(z^2-1)^2}{\gamma^*(z^2-1)^2}, \tag{3.6}$$

where

$$\tilde{\gamma} = \frac{1}{2}\left(\cot^2\hat{\alpha} - \left(\frac{1-h^2}{1+h^2}\right)^2\right), \quad \gamma^* = \frac{1}{2}\left(\cot^2\hat{\alpha} + \left(\frac{1-h^2}{1+h^2}\right)^2\right).$$

This can be shown to map the quarter-circle into the upper half of the $Z$-plane, with $0 \leqslant \mathrm{Re}(z) < 1$ being mapped to $(1+\tilde{\gamma})/\gamma^* \leqslant \mathrm{Re}(Z) < \infty$, $0 \leqslant \mathrm{Im}(z) \leqslant 1$ to $(1+\tilde{\gamma})/\gamma^* \geqslant \mathrm{Re}(Z) \geqslant \tilde{\gamma}/\gamma^*$, and $|z| = 1, 0 < \arg(z) \leqslant \pi/2$ to $-\infty < \mathrm{Re}(Z) < \tilde{\gamma}/\gamma^*$; furthermore, the points $A$ and $B$ are mapped to $Z = \mp 1$ ($A'$ and $B'$) respectively. The flow above $y = f(x)$ maps therefore by analogy to a Sadovskii-type vortex ($S_-$), enclosed by the mapping of the flow below $y = f(x)$ (see figure 2), denoted by $S_+$. Following Moore *et al.* (1988), we may parameterize $S$ by

$$X(\Theta) = -\cos\Theta, \tag{3.7a}$$

$$Y(\Theta) = \sin^3\Theta \sum_{j=0}^{\infty} a_j \cos j\Theta, \quad 0 \leqslant \Theta \leqslant \pi, \tag{3.7b}$$

into which we have already built the requirement that separation and reattachment at $A$ and $B$ respectively should be tangential; however, see § 6 for a further discussion of the parameterization.

Denoting by $W_\pm = U_\pm - \mathrm{i}V_\pm$ the complex velocities in the $S_\pm$ regions of the $Z$-plane, where

$$U_\pm = \frac{\partial\hat{\psi}_\pm}{\partial Y}, \quad V_\pm = -\frac{\partial\hat{\psi}_\pm}{\partial X}, \tag{3.8a,b}$$

we proceed by first extending $U_\pm - \mathrm{i}V_\pm$ analytically across $Y = 0$ by means of

$$U_\pm(X,Y) = U_\pm(X,-Y), \quad V_\pm(X,Y) = -V_\pm(X,-Y).$$

Applying Cauchy's integral theorem to $W_\pm(Z')/(Z'-Z)$ and using the indented contours shown in figure 2 in order to relate the velocity at a point on $S$ to an integral around the boundary of the vortex and its image in the $X$-axis ($\bar{S}$), we

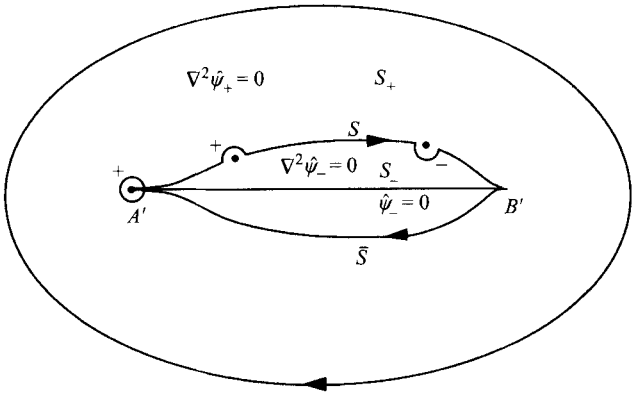


FIGURE 2. Governing equations and indented contours for the application of Cauchy's theorem.

obtain

$$-\pi \mathrm{i} W_+ + \int_{S+\bar{S}} \frac{W_+(Z')\,\mathrm{d}Z'}{Z'-Z} = \int_{\infty} \frac{W_+(Z')\,\mathrm{d}Z'}{Z'-Z}, \tag{3.9a}$$

$$\pi \mathrm{i} W_- + \int_{S+\bar{S}} \frac{W_+(Z')\,\mathrm{d}Z'}{Z'-Z} = 0, \tag{3.9b}$$

where all integrals are taken in the clockwise sense. Consider first the integral on the right-hand side of (3.9*a*). The point $Z = \infty$ corresponds to $z = 1$, which is a stagnation point in the physical plane of the flows $\tilde{\psi}_+$, $\psi_c$ and hence $\hat{\psi}_+$. Furthermore, differentiating (3.6) with respect to $z$ gives

$$\dot{Z}(z) = -\frac{8z(z^2+1)}{\gamma^*(z^2-1)^3}, \tag{3.10}$$

so that, since $\dot{Z}(1)^{-1} = 0$, $Z = \infty$ is a stagnation point of the transformed flow, and hence the integral vanishes; equations (3.9*a*,*b*) may then be amalgamated to give

$$\mp \pi \mathrm{i} W_\pm + \int_{S+\bar{S}} \frac{W_\pm(Z')\,\mathrm{d}Z'}{Z'-Z} = 0. \tag{3.11a,b}$$

Incidentally, the points of the quarter-circle where $\dot{Z}$ vanishes, that is $z = 0, \mathrm{i}$, present no problem, since they are stagnation points at which the complex velocities behave as $z$ and $z - \mathrm{i}$ respectively, so that the complex velocities in the transformed plane at $(1+\tilde{\gamma})/\gamma^*$ and $\tilde{\gamma}/\gamma^*$ are finite. For later use, we note here that the positions of the core centres, in the physical plane, for the two eddies are given by the solutions to

$$\frac{\partial \psi_c}{\partial y} + \mathrm{i}\frac{\partial \psi_c}{\partial x} + W_\pm \dot{Z}(x+\mathrm{i}y) = 0. \tag{3.12a,b}$$

Retaining the earlier notation for the streamfunction as $\hat{\psi}_\pm$ and introducing the velocity potential for the exterior and interior regions as $\hat{\phi}_\pm$, given by

$$U_\pm = \frac{\partial \hat{\phi}_\pm}{\partial X}, \quad V_\pm = \frac{\partial \hat{\phi}_\pm}{\partial Y}, \tag{3.13a,b}$$

we have that on the boundary $S$, where $\hat{\psi}_\pm = -\psi_c(\Theta)$,

$$W_\pm \frac{\mathrm{d}Z}{\mathrm{d}\Theta} = \frac{\mathrm{d}\hat{\phi}_\pm}{\mathrm{d}\Theta} + \mathrm{i}\frac{\mathrm{d}\hat{\psi}_\pm}{\mathrm{d}\Theta} = \frac{\mathrm{d}\hat{\phi}_\pm}{\mathrm{d}\Theta} - \mathrm{i}\frac{\mathrm{d}\psi_c}{\mathrm{d}\Theta}. \tag{3.14a,b}$$

Multiplying (3.11*a*,*b*) by $\mathrm{d}Z/\mathrm{d}\Theta$ and taking the imaginary part subsequently produces

$$\mp\frac{\mathrm{d}\hat{\phi}_{\pm}}{\mathrm{d}\Theta}+\frac{1}{\pi}\int_0^{\pi}\frac{\mathrm{d}\hat{\phi}_{\pm}}{\mathrm{d}\Theta}(\Theta')\mathrm{Im}\left(\frac{\mathrm{d}Z/\mathrm{d}\Theta}{Z(\Theta')-Z(\Theta)}\right)\mathrm{d}\Theta'$$
$$-\frac{1}{\pi}\int_0^{\pi}\frac{\mathrm{d}\hat{\phi}_{\pm}}{\mathrm{d}\Theta}(\Theta')\mathrm{Im}\left(\frac{\mathrm{d}Z/\mathrm{d}\Theta}{\bar{Z}(\Theta')-Z(\Theta)}\right)\mathrm{d}\Theta'$$
$$=\frac{1}{\pi}\int_0^{\pi}\frac{\mathrm{d}\psi_c}{\mathrm{d}\Theta}(\Theta')\mathrm{Re}\left(\frac{\mathrm{d}Z/\mathrm{d}\Theta}{Z(\Theta')-Z(\Theta)}\right)\mathrm{d}\Theta'$$
$$+\frac{1}{\pi}\int_0^{\pi}\frac{\mathrm{d}\psi_c}{\mathrm{d}\Theta}(\Theta')\mathrm{Re}\left(\frac{\mathrm{d}Z/\mathrm{d}\Theta}{\bar{Z}(\Theta')-Z(\Theta)}\right)\mathrm{d}\Theta', \qquad (3.15a,b)$$

two Fredholm equations of the second kind for $\mathrm{d}\hat{\phi}_{\pm}/\mathrm{d}\Theta$. As in Moore *et al.* (1988), the principal value integral may be removed by rewriting the right-hand sides of (3.15*a*,*b*) as

$$\frac{1}{\pi}\int_0^{\pi}\left[\frac{\mathrm{d}\psi_c}{\mathrm{d}\Theta}(\Theta')\mathrm{Re}\left(\frac{\mathrm{d}Z/\mathrm{d}\Theta(\Theta)}{Z(\Theta')-Z(\Theta)}\right)-\frac{\mathrm{d}\psi_c}{\mathrm{d}\Theta}(\Theta)\mathrm{Re}\left(\frac{\mathrm{d}Z/\mathrm{d}\Theta(\Theta')}{Z(\Theta')-Z(\Theta)}\right)\right]\mathrm{d}\Theta'$$
$$+\frac{1}{\pi}\frac{\mathrm{d}\psi_c}{\mathrm{d}\Theta}\log\left|\left(\frac{1-Z(\Theta)}{1+Z(\Theta)}\right)\right|+\frac{1}{\pi}\int_0^{\pi}\frac{\mathrm{d}\psi_c}{\mathrm{d}\Theta}(\Theta')\mathrm{Re}\left(\frac{\mathrm{d}Z/\mathrm{d}\Theta(\Theta)}{\bar{Z}(\Theta')-Z(\Theta)}\right), \qquad (3.16)$$

so that the integrands are bounded for $Z\neq\pm1$; here $\bar{Z}$ denotes the complex conjugate of $Z$.

However, the cusps at $Z=\pm1$ require special treatment which differs from that in Moore *et al.* (1988). In both cases, the velocities at the cusps are finite, and since $\mathrm{d}Z/\mathrm{d}\Theta\sim\Theta$ (or $\pi-\Theta$), we have $\mathrm{d}\tilde{\phi}_{\pm}/\mathrm{d}\Theta\sim\Theta$ (or $\pi-\Theta$). At $Z=\pm1$, the integrals on the left-hand side of (3.15*a*,*b*) are finite, so that the entire left-hand side vanishes. The right-hand side vanishes too, since

$$\frac{\mathrm{d}\psi_c}{\mathrm{d}\Theta}=\frac{\partial\psi_c}{\partial X}\frac{\mathrm{d}X}{\mathrm{d}\Theta}+\frac{\partial\psi_c}{\partial Y}\frac{\mathrm{d}Y}{\mathrm{d}\Theta}$$
$$\sim\sin^2\Theta$$

implies that all the integrands are finite and that the non-integral term vanishes; thence (3.15*a*,*b*) is satisfied identically. Instead, we evaluate (3.11*a*) at the endpoints to obtain, for $S_+$,

$$-(Q_+)_{Z=\pm1}-\int_0^{\pi}Y\frac{\mathrm{d}\hat{\phi}_+}{\mathrm{d}\Theta}\frac{\mathrm{d}\Theta}{|Z\mp1|^2}=\int_0^{\pi}\frac{(X\mp1)}{|Z\mp1|^2}\frac{\mathrm{d}\psi_c}{\mathrm{d}\Theta}\mathrm{d}\Theta. \qquad (3.17a,b)$$

For $S_-$, we appeal to the fact that the cusps are stagnation points of the inviscid flow in the $z$-plane; however, the substitution given by (3.1*a*,*b*) has introduced tangential velocities

$$u_A(\hat{\alpha})=-\frac{1}{\pi}\left(\left(\tfrac{1}{2}\pi-2\hat{\alpha}\right)\cos2\hat{\alpha}-\tfrac{1}{2}\pi+\sin2\hat{\alpha}\log(2\sin2\hat{\alpha})\right), \qquad (3.18a)$$

$$u_B(h)=\frac{1}{\pi}\left(-2h\log h+\frac{1}{2}\left(h-\frac{1}{h^3}\right)\log(1-h^4)\right) \qquad (3.18b)$$

at $A$ and $B$ respectively which must be cancelled out by the tangential velocity

contribution of $\tilde{\psi}_-$. Taking these and transformation (3.6) into account, we arrive at

$$(Q_-)_{Z=-1} = u_A(\hat{\alpha}) \mid \dot{Z}(e^{i\hat{\alpha}}) \mid^{-1} = \frac{u_A(\hat{\alpha})\gamma^* \sin^3 \hat{\alpha}}{4 \cos \hat{\alpha}}, \tag{3.19a}$$

$$(Q_-)_{Z=1} = u_B(h) \mid \dot{Z}(ih) \mid^{-1} = \frac{u_B(h)\gamma^*(1+h^2)^3}{8h(1-h^2)}. \tag{3.19b}$$

To solve (3.15*a*,*b*), we write

$$\frac{d\hat{\phi}_\pm}{d\Theta} = \sin \Theta \sum_{n=0}^{N} c_n^\pm \cos n\Theta \tag{3.20a,b}$$

and require that (3.15*a*,*b*) be satisfied at the points $\Theta_j = j\pi/N, j = 1, .., N-1$. For $\hat{\phi}_+$, (3.17*a*,*b*) provides an extra two conditions for $j = 0, N+1$ ($\Theta_0 = 0, \Theta_N = \pi$) to give a linear system of $N+1$ equations for the $N+1$ unknowns $(c_j^+)_{j=0,..N}$. Expressions (3.19*a*,*b*) do likewise for $(c_j^-)_{j=0,..N}$ with, incidentally, $(Q_-)_{Z=\mp 1}$ given by a routine application of l'Hopital's rule as

$$(Q_-)_{Z=-1} = \lim_{\Theta \to 0} \frac{\dfrac{d\tilde{\phi}_-}{d\Theta} - i\dfrac{d\psi_c}{d\Theta}}{\dfrac{dZ}{d\Theta}} = \sum_{n=0}^{N} c_n^-, \tag{3.21a}$$

$$(Q_-)_{Z=1} = \lim_{\Theta \to \pi} \frac{\dfrac{d\tilde{\phi}_-}{d\Theta} - i\dfrac{d\psi_c}{d\Theta}}{\dfrac{dZ}{d\Theta}} = \sum_{n=0}^{N} (-1)^n c_n^-. \tag{3.21b}$$

The linear systems for $(c_j^\pm)_{j=0,N}$ were solved using LU decomposition and backward substitution. The integrals for these systems were computed using Simpson's rule with adaptive step size, as given by Press *et al.* (1989). Early runs of our code indicated that the integrals on the right-hand side of (3.15*a*,*b*) were particularly sensitive to the integration convergence criterion, but ultimately the condition

$$\left| \frac{I_{n+1} - I_n}{I_n} \right| < 10^{-8} \tag{3.22}$$

was found to be adequate; here, $I_n$ denotes the value of an integral at the $n$th refinement for Simpson's rule and in most cases $n \leqslant 14$. Having found $(c_j^\pm)_{j=0,N}$, and thence the velocity on each side of the free boundary, we define the residual function $R$, based on (3.5), by

$$R(\Theta) = \left(\tilde{Q}_+ + Q_c\right)^2(\Theta) - \Omega^2 \left(\tilde{Q}_- + Q_c\right)^2(\Theta) - Q^2. \tag{3.23}$$

The counting question presents no problem here. Applying (3.23) at the $(N+1)$ collocation points used earlier and noting that $Q$ and $\Omega$ are unknowns, it is clear that if we truncate (3.7*b*) to

$$Y(\Theta) = \sin^3 \Theta \sum_{j=0}^{N-2} a_j \cos j\Theta, \quad 0 \leqslant \Theta \leqslant \pi, \tag{3.24}$$

we will have a nonlinear system of $N+1$ equations

$$R(\Theta_j) = 0, \quad j = 0,..,N, \tag{3.25}$$

in $N+1$ unknowns $(a_0,..,a_{N-2},\Omega,Q)$.

The system was solved using Newton's method, although in view of the lack of an obvious candidate as an initial guess from which iterations could proceed, the following approach was adopted. Noting that the conformal map

$$z \longmapsto \tau = \frac{1+z^2}{1-z^2}$$

transforms the quarter-circle $|z| \leqslant 1$, $0 \leqslant \arg z \leqslant \frac{1}{2}\pi$ in the $z$-plane to the quarter-plane $\mathrm{Re}(\tau) \geqslant 0, \mathrm{Im}(\tau) \geqslant 0$, with the points $A$ and $B$ transformed to $i\cot\hat{\alpha}$ and $(1-h^2)/(1+h^2)$ respectively, consider the curve

$$\left(\frac{\tilde{X}}{(1-h^2)/(1+h^2)}\right)^{2/3} + \left(\frac{\tilde{Y}}{\cot\hat{\alpha}}\right)^{2/3} = 1, \tag{3.26}$$

which has the desired tangency properties at its endpoints on the real and imaginary axis ($\tau = \tilde{X} + i\tilde{Y}$). Noting now that the map $\tau \longmapsto Z = (\tau^2 + \tilde{\gamma})/\gamma^*$ maps this quarter-plane to the upper $Z$-plane, in particular fixing the images of the original points $A$ and $B$ at $-1$ and 1 respectively, we have

$$X = \frac{\tilde{X}^2 - \tilde{Y}^2 + \tilde{\gamma}}{\gamma^*},$$

$$Y = \frac{2\tilde{X}\tilde{Y}}{\gamma^*}.$$

Parameterizing (3.26) by

$$\tilde{X}(\Lambda) = \left(\frac{1-h^2}{1+h^2}\right)\cos^3\tfrac{1}{2}\Lambda,$$

$$\tilde{Y}(\Lambda) = \cot\hat{\alpha}\sin^3\tfrac{1}{2}\Lambda, \quad 0 \leqslant \Lambda \leqslant \pi,$$

we find that

$$a_n = \left(\frac{2-\delta_{0n}}{4\pi\gamma^*}\right)\left(\frac{1-h^2}{1+h^2}\right)\cot\hat{\alpha}\int_0^{\pi}\frac{\cos n\Theta\sin^3\Lambda(\Theta)}{\sin^3\Theta}\,\mathrm{d}\Theta, \tag{3.27}$$

where $\delta_{ij}$ is the Kronecker delta, and $\Lambda(\Theta)$ is determined by solving

$$\gamma^*\cos^3\Lambda - 3\tilde{\gamma}\cos^2\Lambda + 3\gamma^*\cos\Lambda + (3\tilde{\gamma} + 4\gamma^*\cos\Theta) = 0. \tag{3.28}$$

Elementary analysis shows that there is no ambiguity in this prescription for $\Lambda$, since for the range $0 \leqslant \Theta \leqslant \pi$, there is a unique $\Lambda(\Theta)$ for any $0 < \hat{\alpha} < \frac{1}{2}\pi, 0 < h < 1$.

Furthermore, whilst the above provides a plausible initial guess for $(a_j)_{j=0,N-2}$, and thus the free boundary shape, it remains unclear as to what constitutes a good guess for $\Omega$ and $Q$. In view of the form of equation (3.23), it proves convenient to eliminate $\Omega$ and $Q$ and to reduce the system to one of $N-1$ equations. First we note that the converged solution will have the properties that

$$Q_+(\Theta_0) = Q_+(\Theta_N) = Q, \tag{3.29}$$

| | $(\alpha = 0.22, \Omega = 1.144)$ | | | $(\alpha = 0.3, \Omega = 1.961)$ | | $(\alpha = 0.4, \Omega = 1.262)$ | |
|---|---|---|---|---|---|---|---|
| | $N = 32$ | $N = 48$ | $N = 64$ | $N = 32$ | $N = 48$ | $N = 32$ | $N = 48$ |
| $h$ | 0.302633 | 0.302633 | 0.302633 | 0.499999 | 0.499999 | 0.737947 | 0.737947 |
| $Q$ | 0.188137 | 0.188156 | 0.188156 | 0.144984 | 0.144977 | 0.174102 | 0.174102 |
| $a_A$ | 0.101234 | 0.101224 | 0.101217 | 0.212702 | 0.212647 | 0.120234 | 0.120220 |
| $a_B$ | 0.169181 | 0.169033 | 0.169000 | 0.307897 | 0.307922 | 0.157959 | 0.157934 |

TABLE 1. Results of computations for three $(\alpha, \Omega)$ combinations $(N = 32, 48, 64)$

and that for any $M$ $(1 \leqslant M \leqslant N-1)$,

$$\Omega^2 = \frac{Q_+^2(\Theta_M) - Q_+^2(\Theta_0)}{Q_-^2(\Theta_M)}. \tag{3.30}$$

In view of these, the $N-1$ conditions to be iterated for are now

$$Q_+^2(\Theta_0) = Q_+^2(\Theta_N), \tag{3.31}$$

$$Q_+^2(\Theta_j) - \frac{(Q_+^2(\Theta_M) - Q_+^2(\Theta_0))}{Q_-^2(\Theta_M)} Q_-^2(\Theta_j) = Q_+^2(\Theta_0), \quad j = 2, .., N-1 \quad (j \neq M). \tag{3.32}$$

Since the above is valid for any combination of $\hat{\alpha}$ and $h$, we decided to run our code first for many $(\hat{\alpha}, h)$-combinations just to generate $Q_\pm$ values, and then to proceed to iterate on the boundary shape for that combination which best satisfied (3.31). Once this solution had been obtained, the converged $(a_n)$ values were used as an initial guess for a new adjacent $(\hat{\alpha}, h)$-combination; in this way a suite of solutions was generated for $0 < \hat{\alpha} < \frac{1}{2}\pi$, $0 < h < 1$.

## 4. Results

Most of the runs were carried out for $N = 32$, although several additional computations were carried out for $N = 48$ and 64 in order to verify that our results were not dependent on the truncation levels of the Fourier series. Computationally, obtaining a converged solution proved to be very expensive in terms of CPU time: each Newton–Raphson step required the computation of $O(N^3)$ integrals and, with a convergence criterion for the residuals of $10^{-10}$, on average around 10 steps were necessary, requiring a total of around 16 hours. In real time, however, solutions were obtained within an hour by using parallelized code on a Cray supercomputer, thereby making use of the fact that, in the course of one Newton iteration, the most expensive part of the calculation, namely the computation of the integrals, does not need to be carried out sequentially, but can be divided between competing processors.

For $N = 32$, converged solutions were secured for $0.210 \leqslant \alpha \leqslant 0.466$ (where $\alpha = \hat{\alpha}/\pi$, so that $0 \leqslant \alpha \leqslant \frac{1}{2}$). To ascertain the dependence of the results on $N$, for three $\alpha$ values ($\alpha = 0.22, 0.3, 0.4$), we carried out runs for $N = 48$, in each case fixing $\Omega^2$, and iterating for the $(a_n)$ coefficients, $h$ and $q$; one additional run was carried out with $N = 64$ for $\alpha = 0.22$. Table 1 compares the results obtained, for fixed $\alpha$ and $\Omega$, via $h, Q$ and the two cusp constants $a_A$ and $a_B$, given respectively by

$$a_A = 2^{1/3} \sum_{n=0}^{N-2} a_n, \quad a_B = 2^{1/3} \sum_{n=0}^{N-2} (-1)^n a_n. \tag{4.1a,b}$$

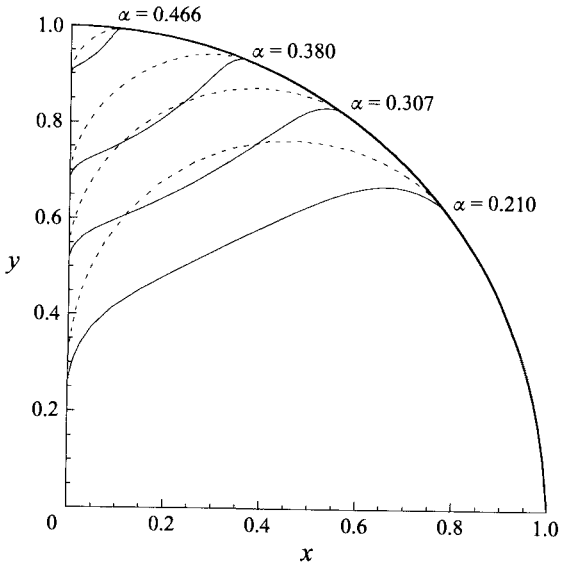


FIGURE 3. Range of free-boundary solutions for $\alpha = 0.210, 0.307, 0.380$ and 0.466.

The results are as expected from Moore *et al.* (1988), with convergence for the cusp constants for different values of $N$ less forthcoming than that for $Q$ and $h$, but sufficiently good to justify using the lowest value of $N$ for further computations in the interests of available computing time. In fact, the most efficient strategy appears to be to obtain converged solutions for $N = 32$, and to use the $(a_n)$ values as the initial guess for higher $N$ for those values of $\alpha$ and $h$ of particular interest, setting the rest of the $(a_n)$ values initially to zero; in this way, the additional computing time required for the solution with $N = 48$ was not significantly greater than the time taken to compute the solution for $N = 32$.

For $\alpha = 0.210, 0.307, 0.380$ and 0.466, we tried to ascertain the range of $h$ for which converged solutions could be obtained; figure 3 shows for each case upper and lower limiting free boundary solutions. In all cases, the solution range for $h$ was roughly $2 \times 10^{-2}$; in particular, the dotted curves correspond to $\Omega = 0$ and therefore constitute upper limits on the position of reattachment. In respect of this, a cautionary word is necessary regarding the reduction of the system to $(N - 1)$ equations, as given by equations (3.29)–(3.32). This simplification obscures the fact that $\Omega^2 \geqslant 0$; indeed, converged 'solutions' were actually obtained for $\Omega^2 \leqslant 0$, although these must be ruled out on the grounds that the streamfunction should be real. In a later version of our code, we chose to prescribe $\alpha$ and $\Omega$, rather than $\alpha$ and $h$, to eliminate this possibility.

The curves of figure 3 are the endpoint solutions of the curves in figure 4, which is a plot of $\Omega$ *vs.* $Q$ for the solutions that were obtained. Throughout these results, it is notable how significantly different the overall shape of the dividing streamline is, even for a small change in $h$. Quantitatively, a change of $O(10^{-2})$ in $h$ yields a change of $O(10^{-1})$ in the maximum height of the curve and an $O(1)$ change in $\Omega$. In all cases, for fixed $\alpha$, $h$ decreases monotonically with $\Omega$. The range of possible $Q$ values lies within a band of width at most 0.1 for each $\alpha$, and it would appear that the $Q \to 0$ limit is simply the case where the free boundary collapses onto the point (0,1). Note also that the values of $Q$ are of the order of magnitude that one would expect by comparison with the solution (3.2) for unseparated flow; in that case, if we define

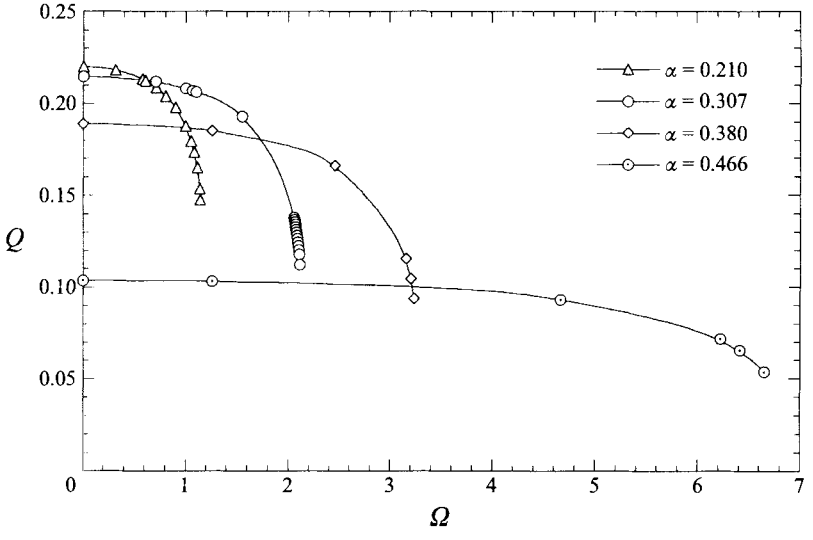


FIGURE 4. Plot of $Q$ *vs.* $\Omega$ for obtained solutions ($\alpha = 0.210, 0.307, 0.380$ and $0.466$).

$Q_{max}$ to be the greatest value of the tangential velocity either on $OA$ or $AB$, we have

$$Q_{max} \leqslant \min\left(\max_{0\leqslant\hat{\alpha}\leqslant\frac{1}{2}\pi} u_A(\hat{\alpha}), \max_{0\leqslant h\leqslant 1} u_B(h)\right). \tag{4.2}$$

The maximum value for $u_A(\hat{\alpha})$ occurs at $\hat{\alpha} = \frac{1}{4}\pi$, whereas that for $u_B(h)$ occurs at the solution of

$$(3 + h^4)\log(1 - h^4) - 4h^4 \log h = 0. \tag{4.3}$$

On computing the relevant values, we find

$$Q_{max} \leqslant \frac{1}{2} - \frac{\log 2}{\pi} \approx 0.279364, \tag{4.4}$$

a little greater than the maximum for the computations for $\alpha = 0.210$.

While the left-hand endpoint constitutes a necessary constraint arising due the form of the equations, as discussed above, the right-hand endpoint appears to be a singular point of the system of equations. By monitoring the Jacobian matrix used for the evaluation of the $(a_n)$ coefficients, we observed that, for fixed $\alpha$, the determinant monotonically decreases from $O(10^6)$ as $\Omega$ increases from zero; for the lower limiting curves shown in figure 3, it is positive and typically $O(10^{-4})$. In fact, we were not able to obtain a converged solution with a negative determinant, although there is no implication that such solutions do not exist. Similarly, the condition number was observed to increase from $O(10^2)$ to $O(10^4)$, indicating a tendency towards ill-conditioning. We also checked the value of the smallest eigenvalue, but found that its real part never changed sign over the range of parameters considered. For the lowest three values of $\alpha$ in figure 4, we carried out further runs, this time with $N = 48$, in order to clarify the phenomenon. In each case, we found that the value of the determinant, which had been $O(10^{-4})$ for $N = 32$, was $O(10^4)$ for $N = 48$. However, monitoring of the condition number for both $N = 32$ and $N = 48$ indicated this to be $O(10^4)$ in both cases, leading us to believe that the singularity is most likely related to the combination of $\alpha$ and $h$. This observation is made more plausible by the fact that in all of the four cases that we have documented in detail, $\mathrm{d}Q/\mathrm{d}\Omega$ near

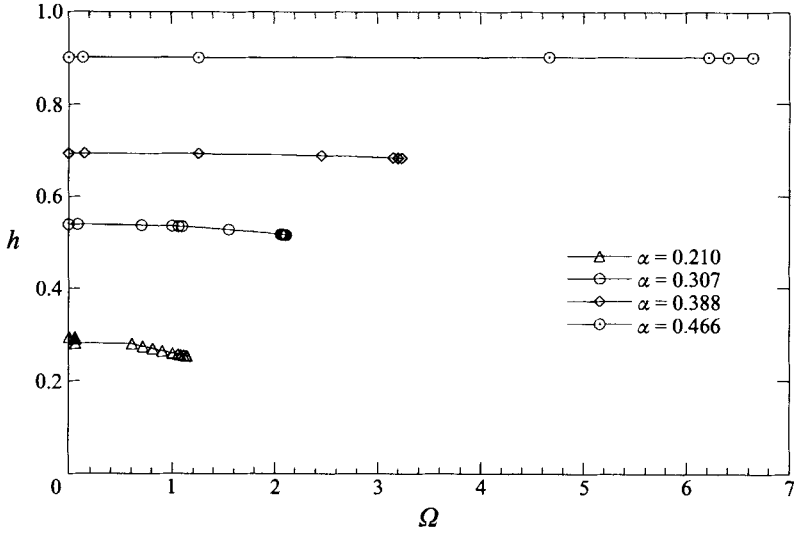


FIGURE 5. Plot of $h$ *vs.* $\Omega$ indicating the parameter ranges within which converged solutions were obtained.

the criticality decreases very rapidly, and in fact may have a turning point. Were this to be the case, there would not be a unique solution to the problem, but instead more than one possible $Q$ solution for some values of $\Omega$, with the failure of the numerical scheme being attributable to this multiplicity.

Figure 5 represents the scope of converged solutions in terms of $\Omega$ and $h$ for the same four $\alpha$ values used in figure 4. Most evident here is the narrowness of the solution band in $h$ for any given $\alpha$, and the wider span of $\Omega$ values as $\alpha$ is increased. Were we to draw a curve passing through the right-hand endpoints of these curves, the region lying to its left, and bounded above below and above by the curves for $\alpha = 0.210, 0.466$ respectively, would constitute the $(h, \Omega)$ domain for which our numerical scheme produced converged results. Although we were not able to generate solutions for $\alpha$ values not in the interval $[0.210, 0.466]$, we shall see that as regards whether any of the above solutions actually do represent the limit of steady laminar flow at high Reynolds number, the above range of $\alpha$ proves adequate.

## 5. Comparison with high-*Re* flow

Now, we examine the above results in the context of the computations, mentioned in § 1, of Vynnycky & Kimura (1994). In fact, we have recomputed their calculations for clockwise flow using a uniform, finer (200 × 200) mesh for $Re$ as high as $9 \times 10^3$, although retaining Patankar's (1980) control-volume method. Since the contour plots for the streamfunction and vorticity are both qualitatively and quantitatively similar, we do not reproduce these here, but concentrate on the numerical values, not documented systematically in the earlier paper, of the positions of separation and reattachment, the ratios of the core streamfunction ($\Psi$) and core vorticity ($\Omega$), as well as the positions of the core centres, $(x_{max}, y_{max})$ and $(x_{min}, y_{min})$ for the primary and secondary eddies respectively, and the position of the dividing streamline. To compare with the method of the present paper, we used the separation point as computed from the Navier–Stokes equations at the highest value of $Re$ ($\alpha = 0.272$ at $Re = 9 \times 10^3$,

| $Re$ | $\alpha$ | $h$ | $\Psi$ | $\Omega$ | $x_{max}$ | $y_{max}$ | $x_{min}$ | $y_{min}$ | $a_A$ | $a_B$ |
|---|---|---|---|---|---|---|---|---|---|---|
| 1000 | 0.294 | 0.578 | 0.028 | 0.320 | 0.485 | 0.349 | 0.120 | 0.795 | - | - |
| 2000 | 0.281 | 0.552 | 0.042 | 0.481 | 0.473 | 0.358 | 0.102 | 0.803 | - | - |
| 3000 | 0.278 | 0.540 | 0.051 | 0.539 | 0.467 | 0.365 | 0.104 | 0.823 | - | - |
| 4000 | 0.274 | 0.532 | 0.056 | 0.597 | 0.465 | 0.365 | 0.106 | 0.838 | - | - |
| 5000 | 0.274 | 0.529 | 0.060 | 0.640 | 0.464 | 0.369 | 0.107 | 0.842 | - | - |
| 6000 | 0.273 | 0.526 | 0.063 | 0.684 | 0.462 | 0.372 | 0.107 | 0.847 | - | - |
| 7000 | 0.271 | 0.524 | 0.065 | 0.715 | 0.462 | 0.372 | 0.107 | 0.848 | - | - |
| 8000 | 0.272 | 0.522 | 0.068 | 0.748 | 0.459 | 0.376 | 0.108 | 0.852 | - | - |
| 9000 | 0.272 | 0.521 | 0.069 | 0.777 | 0.459 | 0.376 | 0.108 | 0.852 | - | - |
| analytical | 0.272 | 0.464 | 0 | 0 | 0.445 | 0.386 | 0.133 | 0.866 | 0.077 | 0.148 |
| analytical | 0.272 | 0.460 | 0.084 | 0.750 | 0.448 | 0.382 | 0.139 | 0.859 | 0.084 | 0.158 |
| analytical | 0.272 | 0.459 | 0.093 | 0.800 | 0.449 | 0.382 | 0.140 | 0.858 | 0.085 | 0.159 |
| analytical | 0.272 | 0.458 | 0.103 | 0.866 | 0.449 | 0.381 | 0.142 | 0.857 | 0.087 | 0.162 |
| analytical | 0.272 | 0.433 | 0.518 | 1.735 | 0.498 | 0.333 | 0.206 | 0.779 | 0.270 | 0.415 |

TABLE 2. Summary of results for high Reynolds number computations and five coupled Batchelor flow solutions for $\alpha = 0.272$

but see its dependence on $Re$ in table 2) as input for the inviscid equations; as before, we generated a suite of solutions for this value of $\alpha$ for different $\Omega$ values.

Table 2 summarizes the dependence of $\alpha$, $h$, $\Psi$, $\Omega$, $x_{max}, y_{max}, x_{min}$ and $y_{min}$ on $Re$ for $10^3 \leqslant Re \leqslant 9 \times 10^3$. The data towards the bottom are for the inviscid solutions for $\alpha = 0.272$, the first of which has the property that $\Omega = 0$, so that $\Psi = 0$. The last row contains the data for the highest value of $\Omega$ that we could compute, with the intervening rows containing data for $\Omega$ close to that found for the Navier–Stokes computations. The positions of the core centres are obtained by solving (3.12*a*,*b*) for $W_{\pm}$ using Newton's method. Furthermore, we plot in figure 6 the location of the dividing free streamline for $Re = 3, 6, 9 \times 10^3$ and for the two extreme inviscid solutions of table 2. Whilst agreement is by no means perfect, there are several encouraging trends. The overall form of the dividing streamline for which $\Omega = 0$ is similar to those for the full computations, with the greatest discrepancy near the point of reattachment where the streamlines have infinite gradient; however, it is reassuring to note that the value of $h$, which is consistently larger for the Navier–Stokes solutions than for the inviscid solutions, is found to decrease with $Re$. The positions of the cores as given by the two methods also agree well, all the more so for the main eddy. Lastly, while the $\Omega = 0$ curve provides the best agreement in terms of $h$, the intermediate curves, which differ in $h$ from the $\Omega = 0$ curve by $O(10^{-3})$, provide better agreement for $\Psi, x_{max}$ and $y_{max}$. For the inviscid solutions, we have also given the values of the cusp constants $a_A$ and $a_B$; these are both found to decrease uniformly with $\Omega$. This appears to be a trend in the right direction, in the sense that the cusp constant at separation of the inviscid solution which is the limit as $Re \to \infty$ of the Navier–Stokes solution should be $a_A = 0$; on the other hand, since the minimum value was obtained for $\Omega = 0$, there is clearly no further possibility of obtaining lower values of $a_A$ for this value of $\alpha$ with the present parameterization.

## 6. Conclusion

We have considered Batchelor flows in a confined quarter-circular cavity. Guided by earlier high Reynolds number computations (Vynnycky & Kimura 1994), which indicated the presence of a primary and a secondary eddy, we have posed a free-

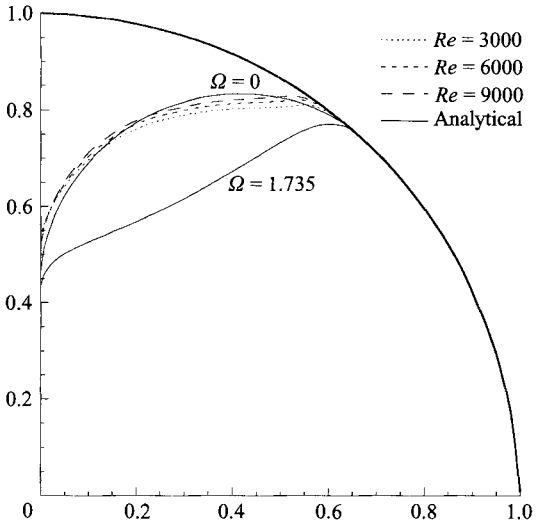


FIGURE 6. The dividing streamline for $Re = 3, 6, 9 \times 10^3$ and limiting Batchelor flows for $\alpha = 0.272$.

boundary problem involving two eddies within the cavity, each of different constant vorticity, with the aim of constructing an inviscid solution which might plausibly represent the limit of infinite Reynolds number flow for this configuration. The fact that both eddies are confined and rotational constitutes the essential difference between this problem and that of external flow past a bluff body. Recasting the problem as a Fredholm integral equation, we have obtained numerically a two-parameter family of solutions; these parameters may be viewed as any two of the following: the separation angle ($\alpha$); the reattachment point ($h$); the ratio of the core vorticities ($\Omega$); and the slip velocity at separation and reattachment of the main eddy ($Q$). We have found that arbitrary prescriptions of $\alpha$ and $h$ do not, in general, lead to numerically obtainable solutions, but that for fixed $\alpha$ we were only able to find solutions for a range in $h$ of width $O(10^{-2})$; for such a range, the value of $Q$ changes by $O(10^{-1})$ and that of $\Omega$ by $O(1)$. For all solutions, for fixed $\alpha$, $Q$ increases and $\Omega$ decreases with increasing $h$. The width of the band in $h$ was found to be constrained by two seemingly unrelated phenomena: if $h$ is too great, the requirement that $\Omega^2 > 0$ is violated, whereas if $h$ is too small, a vanishing determinant appears in the Jacobian matrix for Newton's method. Furthermore, for each of the $\alpha$ values considered, a value of $h$ was found corresponding to $\Omega = 0$; this constitutes a limiting solution corresponding to the decoupling of the eddies, with the secondary eddy stagnant.

The range of $\alpha$ for which solutions were found encompasses the value predicted by high Reynolds number computations, and it is natural to ask whether any of the coupled Batchelor flows found actually approximate to the results of these computations. This was done by using as input for the Batchelor flows the value of $\alpha$ for $Re = 9 \times 10^3$ and generating a family of solutions for different $h$ as explained before. We have found encouraging agreement in terms of the position of the dividing streamline. Furthermore, trends in the value of the reattachment position and the main core centre for increasing $Re$ lend support to the claim that the two-eddy model developed here does show significant promise as regards determining the flow in the infinite-$Re$ limit. However, several further issues must first be borne in mind, as follows.

First, there may be doubt as to whether the results of the Navier–Stokes computations presented actually show any asymptotic limiting behaviour for the range of

Reynolds numbers shown here; in particular, the increase in the values of $\Psi$ and $\Omega$ in table 2 does not provide conclusive evidence that such a limit has been reached. Linear extrapolation of $\Psi$ and $\Omega$ against $Re^{-1/2}$, not presented here, based on the data obtained nominally indicates that, as $Re^{-1/2} \to 0$, $\Psi \approx 0.1, \Omega \approx 1.2$, values which are significantly higher than those actually computed. The issue might therefore be resolved either by computations at much higher Reynolds numbers, assuming steady solutions exist, or the closure of the asymptotic model to be discussed below. Second, in view of the fact that the inviscid problem treated here does not even include the boundary condition which drives the flow in the full equations, there does seem to be scope for ambiguity when comparing methods. For instance, it is likely that changing the flow-driving boundary condition will influence each of the data quantities in table 2. However, subject to the modifications to be discussed in the next paragraph and in view of the way we used $\alpha$ and $\Omega$ to 'fit' to a high-$Re$ solution, it is at least clear that this ambiguity manifests itself at the inviscid level in the fact that $\alpha$ and $h$ (or equally $\Omega$) must be prescribed *a priori* for a well-posed problem; thus, a model including this lost boundary condition should close the problem satisfactorily.

In relation to this and to the counting argument for the discretized inviscid equations, as explained in § 2, it would be preferable, if the Batchelor flow model is ever to be incorporated into an asymptotic treatment of the Navier–Stokes equations for $Re \gg 1$ for the problem formulated in Vynnycky & Kimura (1994), that $\alpha$ and $h$ also be unknowns to be determined. This would require supplementary conditions, in addition to Bernoulli's equations; one possibility would be to impose a continuous curvature condition at separation, as is done by selecting the appropriate curve from Kirchhoff's free-streamline theory for external bluff body flow. This has not been done here, since the parameterization (3.7*a*, *b*) gives only tangential separation, which is all that the inviscid theory requires; the curvature in all cases has been infinite, and it would be of interest to see whether this suggested extra condition will improve agreement between the predictions for the dividing streamline. Certainly, at the cusp level, a parameterization which takes into account both continuous gradient and curvature would automatically give $a_A = 0$, giving better agreement than in § 5 between the inviscid high-$Re$ solutions at the separation point. One more condition would still be required to pin down $h$, or equivalently $Q$ or $\Omega$. Tentatively speaking, this appears to come from a condition on the viscous flow, following either Riley (1981) or Vynnycky (1994), although with significant modification since, in principle, there would be two coupled periodic boundary layers, and therefore a condition on each of $\omega_+$ and $\omega_-$ to determine $\Omega$, possibly uniquely. Another concern here is the possible multiplicity of inviscid solutions speculated upon in § 4, which seems to go against our physical expectation that there should be a unique solution to the problem. One might surmise that the requirements of the boundary-layer theory will settle this also, as would be the case were the necessary computations to produce a value of $\Omega$ that is not near the critical region where $|\,\mathrm{d}Q/\mathrm{d}\Omega\,|$ becomes large, as is suggested by the Navier–Stokes computations presented here.

However, it is perhaps this incorporation of a boundary-layer structure into an asymptotic treatment of the problem presented here that presents the greatest obstacle. Although the high Reynolds number computations did not indicate any more than two eddies, there is a possibility that secondary separation will occur at the no-slip boundary on the smaller-eddy side of the inviscid separation point for the boundary-layer equations, a situation which would wreck the two-eddy model for $\Omega \neq 0$; for $\Omega = 0$, we may have the possibility that the position of the dividing streamline is satisfactorily predicted, even though the subsidiary flow is effectively neglected.

## REFERENCES


BATCHELOR, G. K. 1956*a* On steady laminar flow with closed streamlines at large Reynolds number. *J. Fluid Mech.* **1**, 177–190.

BATCHELOR, G. K. 1956*b* A proposal concerning laminar wakes behind bluff bodies at large Reynolds numbers. *J. Fluid Mech.* **1**, 388–398.

BRUNEAU, C.-H. & JOURON, C. 1990 An efficient scheme for solving steady incompressible Navier-Stokes equations. *J. Comput. Phys.* **89**, 389–413.

BURGGRAF, O. R. 1966 Analytical and numerical studies of the structure of steady separated flows. *J. Fluid Mech.* **24**, 113–157.

CHERNYSHENKO, S. I. 1984 *Izv. Akad. Nauk SSR, Mekh. Zhidk Gaza* **2**, 40–45. (Available in English as 'The calculation of separated flows of low-viscosity liquids using the Batchelor model'. *Royal Aircraft Establishment Library Transl.* 2133.)

CHERNYSHENKO, S. I. 1993 Stratified Sadovskii flow in a channel. *J. Fluid Mech.* **250**, 423–431.

FORNBERG, B. 1985 Steady viscous flow past a circular cylinder up to Reynolds number 600. *J. Comput. Phys.* **61**, 297–320.

GIANNAKIDIS, G. 1993 Prandtl-Batchelor flow in a channel. *Phys. Fluids* A **5**, 863–867.

HADDON, E. W. & RILEY, N. 1985 On flows with closed streamlines. *J. Engng Maths* **19**, 233–246.

KUWAHARA, K. & IMAI, I. 1969 Steady, viscous flow within a circular boundary *Phys. Fluids Supplement II* **12**, 94–101.

LYNE, W. H. 1970 Unsteady viscous flow in a curved pipe. *J. Fluid Mech.* **45**, 13–31.

MOORE, D. W., SAFFMAN, P. G. & TANVEER, S. 1988 The calculation of some Batchelor flows: The Sadovskii vortex and rotational corner flow. *Phys. Fluids* **31**, 978–990.

PATANKAR, S. V. 1980 *Numerical Heat Transfer and Fluid Flow.* Hemisphere.

PIERREHUMBERT, R. T. 1980 A family of steady, translating vortex pairs with distributed vorticity. *J. Fluid Mech.* **99**, 129–143.

PRESS, W. H., FLANNERY, B. P., TEUKOLSKY, S. A. & VETTERLING, W. T. 1989 *Numerical Recipes: The Art of Scientific Computing.* Cambridge University Press.

RILEY, N. 1981 High Reynolds number flows with closed streamlines. *J. Engng Maths* **15**, 15–27.

SADOVSKII, V. S. 1971 Vortex regions in a potential stream with a jump of Bernoulli's constant at the boundary. *Appl. Math. Mech.* **35**, 773–779.

SAFFMAN, P. G. & TANVEER, S. 1984 Prandtl-Batchelor flow past a flat plate with a forward-facing flap. *J. Fluid Mech.* **143**, 351–365.

SCHREIBER, R. & KELLER, H. B. 1983 Driven cavity flows by efficient numerical techniques. *J. Comput. Phys.* **49**, 310–333.

SMITH, F. T. 1985 A structure for laminar flow past a bluff body at high Reynolds number. *J. Fluid Mech.* **155**, 175–191.

SMITH, F. T. 1986 Concerning inviscid solutions for large-scale separated flows. *J. Engng Maths* **20**, 271–292.

SMITH, J. H. B. 1982 The representation of planar separated flow by regions of uniform vorticity. In *Vortex Motion*, pp. 157–172. Vieweg.

TURFUS, C. 1993 Prandtl-Batchelor flow past a flat plate at normal incidence in a channel - inviscid analysis. *J. Fluid Mech.* **249**, 59–72.

VANKA, S. P. 1986 Block-Implicit multigrid solution of Navier Stokes equations in primitive variables. *J. Comput. Phys.* **65**, 138–158.

VYNNYCKY, M. 1994 On the uniform vorticity in a high Reynolds number flow. *J. Engng Maths* **28**, 129–144.

VYNNYCKY, M. & KIMURA, S. 1994 An investigation of recirculating flow in a driven cavity. *Phys. Fluids* **6**, 3610–3620.